JOURNAL OF MATERIALS SCIENCE 26 (1991) 2954–2960

Mechanical behaviour of chemical vapour infiltration-processed two- and three-dimensional nicalon/SiC composites

J.-M. YANG, W. LIN, C. J. SHIH, W. KAI, S. M. JENG
Department of Materials Science and Engineering, School of Engineering and Applied Science, University of California, Los Angeles, CA 90024, USA

C. V. BURKLAND
The Amercom, Inc., Chatsworth, CA 91311, USA

The effect of two different fibre architectures on the mechanical properties of the Nicalon fibre-reinforced SiC composites processed by chemical vapour infiltration has been investigated. The microstructure, flexural strength, fracture toughness and failure mechanisms of both two-dimensional woven laminate and three-dimensional braided composites were characterized. It was found that the fibre placement in the preform will not only affect the infiltration of the SiC matrix, but also the mechanical property and failure behaviour of the composite. A strong, tough and damage-tolerant SiC matrix composite can be fabricated through the combination of a three-dimensional braided integrated fibre network and chemical vapour infiltration processing.

1. Introduction

Continuous fibre-reinforced ceramic matrix composites processed by chemical vapour infiltration (CVI) have been under intensive development for various high temperature structural applications. They offer several attractive features including high strength and modulus, improved fracture toughness, light weight, low thermal expansion coefficient and high thermal conductivity which contribute to good thermal shock resistance, and high temperature stability in chemical and oxidative environments. Potential applications of these promising composites include turbine and automotive engine components, advanced structures for hypersonic aircraft and spacecraft, etc. Various refractory ceramic matrices including SiC, Al_2O_3, Si_3N_4, B_4C, TiC, and BN have been successfully deposited on to the porous fibre preform [1–11]. A major advantage of the CVI technique is that it is performed at temperatures lower than those used for conventional powder processing; thus, there is less likelihood of mechanical damage or chemical attack of the fibre. Another attractive feature of this technique is that the shape and dimension of the infiltrated structure are virtually identical to those of the initial fibre preform. Therefore, it has the potential for near net shape manufacturing of complex structural components. Furthermore, the fibre/matrix interface chemistry can be tailored for fibre protection and control of bond strength by varying the deposition parameters.

It has been shown that the performance of the CVI-processed ceramic composites are strongly affected by the fibre architecture, the fibre/matrix interface, the matrix composition and processing parameters [8–11]. Key processing variables such as temperature, pressure, reagent concentration and gas flow rate will influence the infiltration and development of the matrix microstructure, and therefore the mechanical properties of the composites. For example, crystalline perfection and grain size of the SiC normally increase with increasing deposition temperature. However, it is desirable that the CVI process is carried out at lower temperatures to enhance infiltration. Therefore, the successful achievement of in-depth infiltration of silicon carbide into a complex porous structure requires a knowledge of the thermodynamics and kinetics of chemical vapour deposition on surfaces combined with mass transport into pores [4, 5].

The fibre architecture is another important parameter which will significantly affect the strength, toughness and failure of the composites. The preforms are generally in the form of unidirectional arrays, woven fabrics, or multidirectional textile structures [12–14]. Various unidirectional and two-dimensional (2-D) woven fabric-reinforced ceramic matrix composites densified by the CVI-technique with improved properties have been reported [4–11]. More recently, the development of various novel fibre architectures offer promising potential for reinforcing ceramic matrix composites with performance superior to that of the conventional laminated composites. For example, a three-dimensional (3-D) braided structure not only offers a multidirectional reinforcement, but also has the capability for the direct formation of complex structural shapes in an integrated manner [12]. Furthermore, the flexibility in fibre placement and fibre-

0022–2461/91 $03.00 + .12

hybridization permits the composite to be tailored to provide the desired properties required for a given component.

The purpose of this paper is to characterize the strength and toughness of the Nicalon fibre-reinforced SiC composites with two different reinforcement geometries. The failure mode and toughening mechanisms under various thermo-mechanical loadings were also investigated.

2. Experimental procedure

2.1. Materials

Two types of Nicalon fibre preforms, a 3-D braided structure, and a 2-D plain-weave fabric with $[0/30/60/90]_{2S}$ stacking sesquence, were used as shown in Fig. 1 [13]. The 3-D braided preform has a 1 × 1 braiding pattern, and the average angle between the fibre bundles and the braiding axis was approximately ± 20° [12]. The preforms were densified simultaneously with the SiC matrix by the chemical vapour infiltration process in a hot-wall reactor using methyltrichlorosilane (MTS) as precursor. Prior to matrix densification, the fibre preforms were coated with a thin layer of pyrolytic carbon to modify the interface chemistry. In addition, the coating may protect the fibres from damage and environmental attack during processing. The CVI processing was carried out at Amercom, an Atlantic Research Corporation company. The resultant 3-D braided Nicalon/SiC composite panel has a density of 2.6 g cm^3, contains 32% fibre volume fraction with a residual porosity of 10.94%. The 2-D woven laminate composite contains 35 v/o of fibres, and has a slightly lower density (2.3 g/cm^3) with close to 15% of porosity.

2.2. Mechanical Testing

The CVI-processed SiC matrix composites were subjected to various mechanical tests to evaluate the effect of fibre architectures on their mechanical performance. In order to study the thermal stability of the composite, some of the specimens were thermally exposed at 1200 °C for 100 hours at ambient atmosphere. The flexural strengths of the as-processed and heat-treated specimens were measured using a four-point bend test in an Instron testing machine with a crosshead speed of 0.5 mm/s. The specimen has a dimension of 3 × 3 × 50 mm with the inner and outer span of 20 and 40 mm, respectively. The load was introduced perpendicular to the braiding direction (1–2 plane) for the braided composite, and perpendicular to the layers of the fabric (1–2 plane) for the woven laminate composite. The dynamic flexural strength and energy-absorbing capability was measured using an instrumented Charpy impact test with a speed of 1.95 m/s on an unnotched specimen (5 × 5 × 50 mm).

The fracture toughness was measured using a single edge notched-beam technique in three-point bending at a crosshead speed of 0.5 mm/s. The specimen has a dimension of 5 × 5 × 25 mm with a lower span of 18.75 nmm. The notches were perpendicular to both the (1–2) and (1–3) planes for the 3-D braided composite, and perpendicular to both the (1–2) and (1–3) planes for the 2-D woven laminate composite. The notches were introduced using a 0.25 mm thick diamond blade and had a depth of one-third of the specimen thickness. The fracture toughness was calculated according to the procedures described in ASTM E399 except that the maximum load was used.

All the tests were conducted at room temperature, and a minimum of ten specimens were used in each test. X-ray diffraction analysis was used to identify the phase present in the composite before and after thermal exposure. Optical and scanning electron microscopy was used to study the fracture characteristics of the composites.

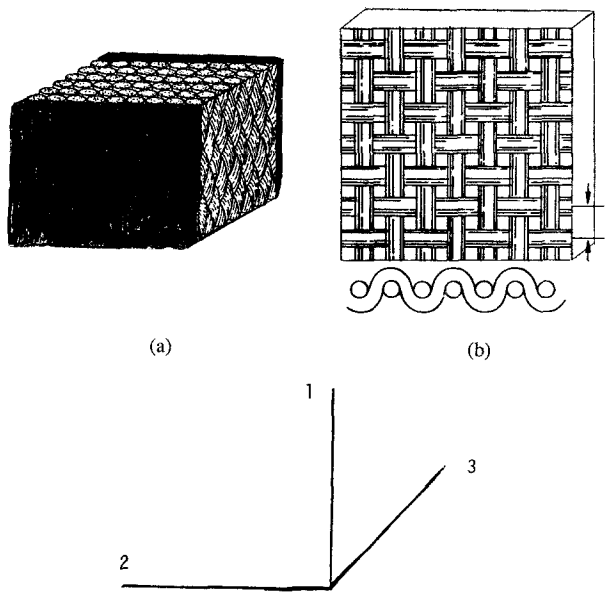

Figure 1 The geometry of (a) 3-D braided and (b) 2-D woven structures

3. Results

The optical micrographs for the CVI-processed Nicalon/SiC composites with 3-D braided and 2-D woven structures are shown in Figs 2 and 3, respectively. These micrographs clearly show that the silicon carbide matrix is uniformly deposited within the pores on each Nicalon fibre in the bundle. However, it is apparent that the infiltration of the SiC matrix depends on the features of the pore network in the preform structure. In the case of the 2-D woven Nicalon/SiC laminate composite, large voids were still present between fabric layers and could not be filled during infiltration. In the case of the 3-D braided Nicalon/SiC composite, significantly fewer and smaller voids were found. However, some large voids were still present at the bundle cross-over.

The flexural strength for both 3-D braided and 2-D woven laminate Nicalon/SiC composites are listed in Table I. The as-processed 3-D braided composite with load applied perpendicular to the braiding direction (1–2 plane) has an averaged flexural strength of 692 MPa. The typical stress–deflection curves for both as-processed and heat-treated composites are shown

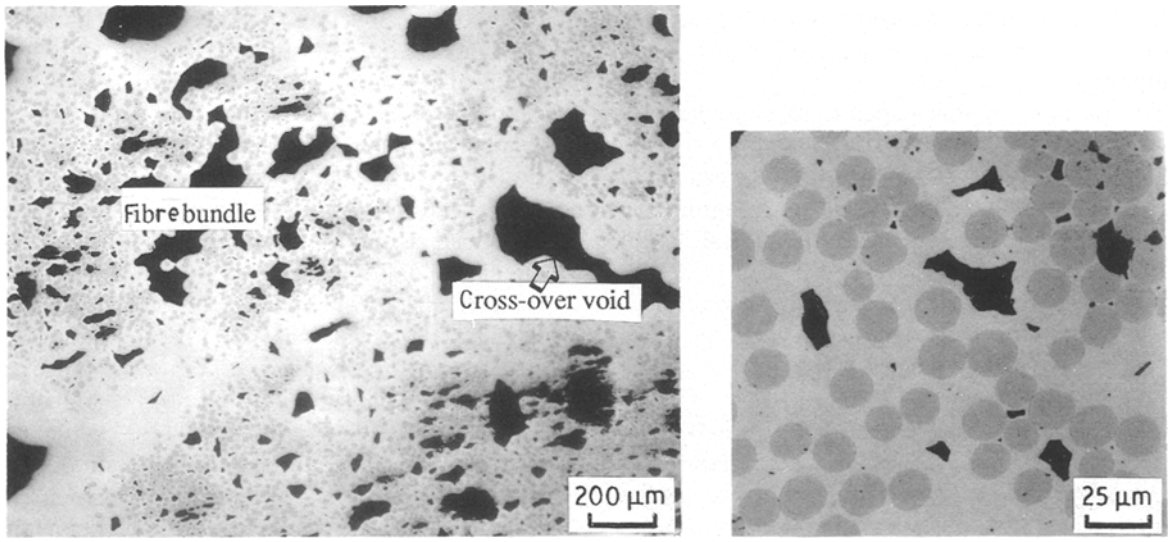

Figure 2 The optical micrograph of the as-received 3-D braided Nicalon/SiC composite.

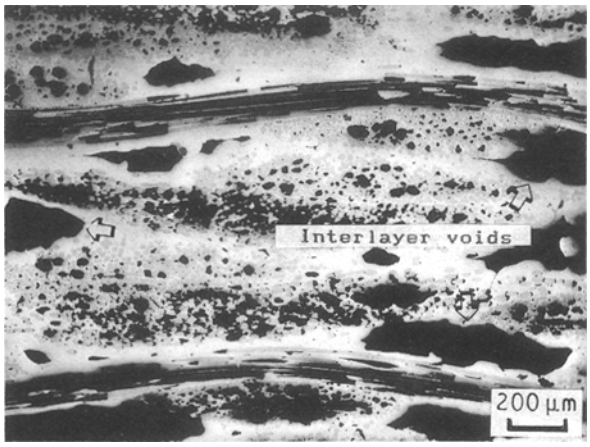

Figure 3 The optical micrograph of the as-received 2-D woven laminate Nicalon/SiC composite.

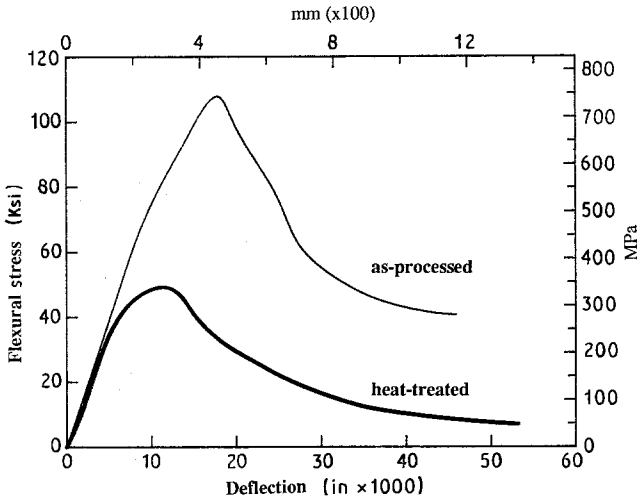

Figure 4 The typical flexural stress-deflection curve for both as-processed and heat-treated 3-D braided composites.

in Fig. 4. The composite exhibited an initial linear elastic behaviour followed by a non-linear stress–deflection behaviour until the maximum stress is reached. The non-linearity is due to the progressive cracking of the matrix together with partial debonding between fibres and matrix. Ultimately, the matrix is severely cracked, the fibre can no longer carry the load, and fractures; this corresponds to the maximum stress in the load–deflection curve. However, the composite continued to carry the load after the ultimate stress was reached because of the continued fibre pull-out from the matrix. After thermal exposure at 1200 °C for 100 hours in the oxidizing environment, the flexural strength decreased to 350 MPa. Nontheless, the composite still exhibited a ductile stress–deflection behaviour. It appeared that the flexural modulus remained almost unchanged after thermal exposure as indicated in the initial slope of the stress–deflection curves. The 2-D woven laminate has an averaged flexural strength of 330 MPa, which is

TABLE I Mechanical Property of Nicalon/SiC composites

	density ($g\,cm^{-3}$)	Flexural strength (MPa)	Fracture toughness (MPa $m^{1/2}$) 1–3	1–2
3-dimensional braided				
as-received	2.6	692 ± 39	29.8 ± 2.5	18.1 ± 0.7
heat-treated at 1200 °C for 100 h	2.6	345 ± 6	13.3 ± 1.0	10.0 ± 1.2
2-dimensional woven				
as-received	2.3	326 ± 16	16.2 ± 1.7	11.9 ± 0.7
heat-treated at 1200 °C for 100 h	2.3	170 ± 28	8.2 ± 0.5	6.8 ± 1.0

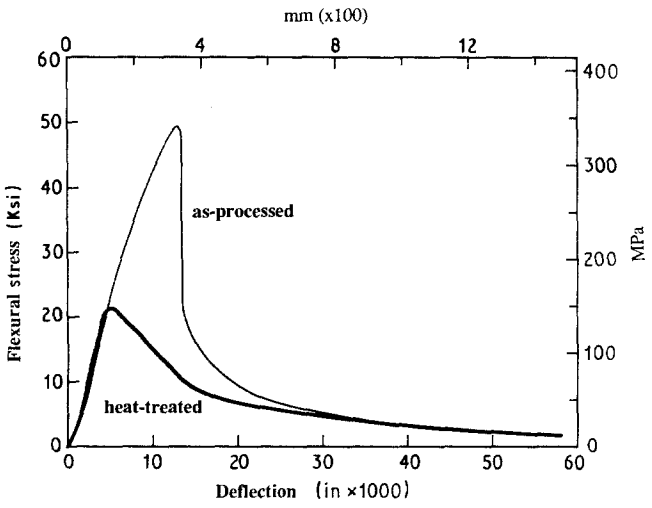

Figure 5 The typical flexural stress-deflection curve for both as-processed and heat-treated 2-D woven laminate composites.

similar to the results reported elsewhere [8]. After thermal exposure, the flexural strength dropped to 170 MPa. The typical stress–deflection curves of the 2-D woven laminate composites exhibited similar non-catastrophic stress–deflection behaviour as shown in Fig. 5. Nevertheless, the flexural strength of the 2-D woven laminate composite dropped faster than that of the 3-D braided composite after the ultimate stress was reached.

The flexural stress versus deflection curve obtained from the instrumented Charpy impact test for both 3-D braided and 2-D woven laminate composites is shown in Fig. 6. The areas under the stress (load)–deflection curve represent the amount of energy the composite can absorb during crack initiation and propagation. It is clear that both types of composites showed a non-catastrophic failure behaviour with considerable inelastic deformation before the maximum load was reached, and were capable of absorbing appreciable amount of energy under dynamic loading. The average dynamic flexural strengths of the as-processed 3-D braided and 2-D woven laminate composites were 670 MPa and 358 MPa, respectively. The 3-D braided composite absorbed more energy

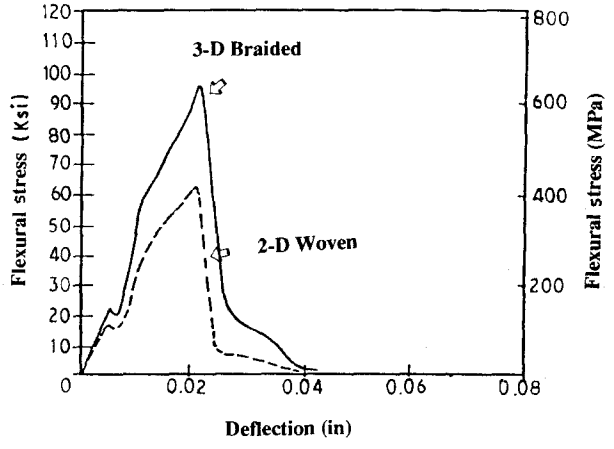

Figure 6 The dynamic flexural stress-deflection curve for both 3-D braided and 2-D woven laminate composites.

prior to final failure than that of the 2-D woven laminate composite.

The fracture toughness values of the as-processed and heat-treated Nicalon/SiC composites tested at room temperature are also listed in Table I. The as-processed 3-D braided composite has an average fracture toughness of 29.8 MPa $m^{1/2}$ and 18 MPa $m^{1/2}$ for a crack propagated perpendicular to the (1–3) and (1–2) plane, respectively. An exceptionally high fracture toughness was achieved in a CVI-SiC matrix composite with the 3-D braided structure as compared with that of the monolithic SiC (3–5 MPa $m^{1/2}$). After thermal exposure at 1200 °C for 100 hours in an oxidizing atmosphere, the fracture toughness values decreased to 13.3 MPa $m^{1/2}$ and 8 MPa $m^{1/2}$, respectively. The as-processed 2-D woven laminate composite has an average fracture toughness of 16.2 MPa $m^{1/2}$ and 11.9 MPa $m^{1/2}$ for a crack propagated perpendicular to the (1–3) and (1–2) plane, respectively. After thermal exposure, the fracture toughness values decreased to 8.2 MPa $m^{1/2}$ and 6.8 MPa $m^{1/2}$, respectively. Both the 2-D woven and 3-D braided composites exhibited a non-catastrophic load–deflection behaviour. They also exhibited an anisotropic behaviour in crack-propagation resistance for both as-processed and heat-treated specimens.

The crack propagation characteristics of both 3-D braided and 2-D woven laminate composites are shown in Figs 7 and 8, respectively. The crack propagated mainly along the pre-notch direction for both types of composites, and no significant lateral cracking was observed. Scanning electron microscopy (SEM) fractographs for 3-D braided and 2-D woven laminate Nicalon/SiC composites are shown in Figs 9 and 10, respectively. A significant amount of fibre pull-out was observed on the fracture surfaces for both types of composites which leads to the improved fracture toughness and strain-to-failure. The fracture surface of the as-processed 2-D woven laminate and 3-D braided composite subjected to impact loading is shown in Fig. 11. Much less fibre pull-out together with severe matrix cracking was observed.

4. Discussion

The above results clearly indicate that the strength, fracture toughness and impact energy-absorbing capability of an SiC ceramic composite with 3-D braided reinforcement is superior to that of a 2-D woven laminate composite. It is apparent that the 3-D braided composite is more damage-tolerant under both static and dynamic loadings. This is due to the fact that the braided structure has an integrated 3-D intertwined fibre network which offers a better resistance to crack propagation. A similar structural strengthening/toughening effect provided by a 3-D braided Nicalon-fibre architecture in a lithium aluminosilicate (LAS III) glass ceramic matrix has also been demonstrated [15]. Obviously, the effect of fibre placement affects the failure behaviour and toughening mechanisms of the composites. Microscopic observation of the specimens fractured in flexure indicated that both types of composites failed at the tensile

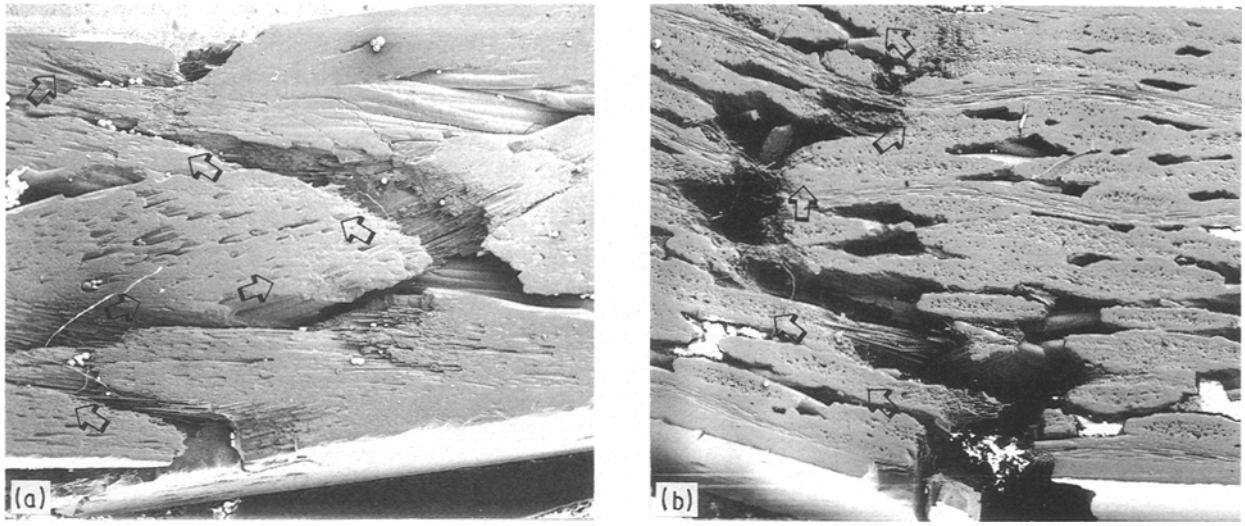

Figure 7 The crack propagation pattern of the as-processed (a) 3-D braided, (b) 2-D woven laminate Nicalon/SiC composite.

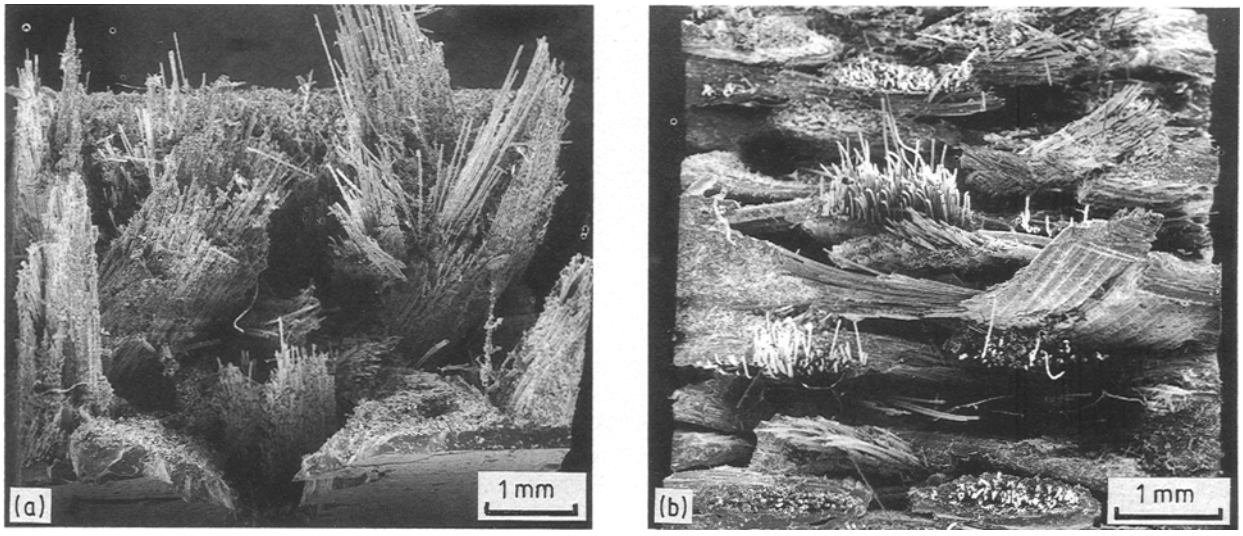

Figure 8 The fracture surface of the as-processed (a) 3-D braided, (b) 2-D woven laminate composite.

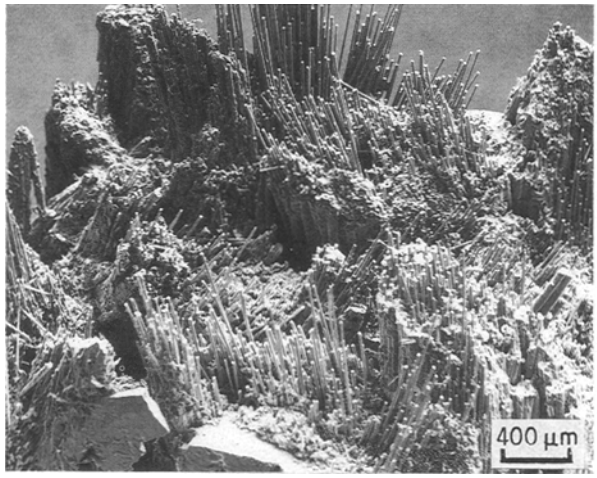

Figure 9 The SEM fractograph of the as-processed 3-D braided Nicalon/SiC composite.

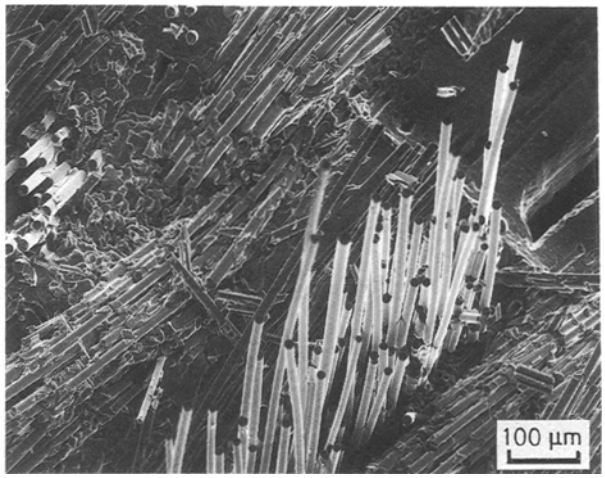

Figure 10 The SEM fractograph of the as-processed 2-D woven laminate Nicalon/SiC composite.

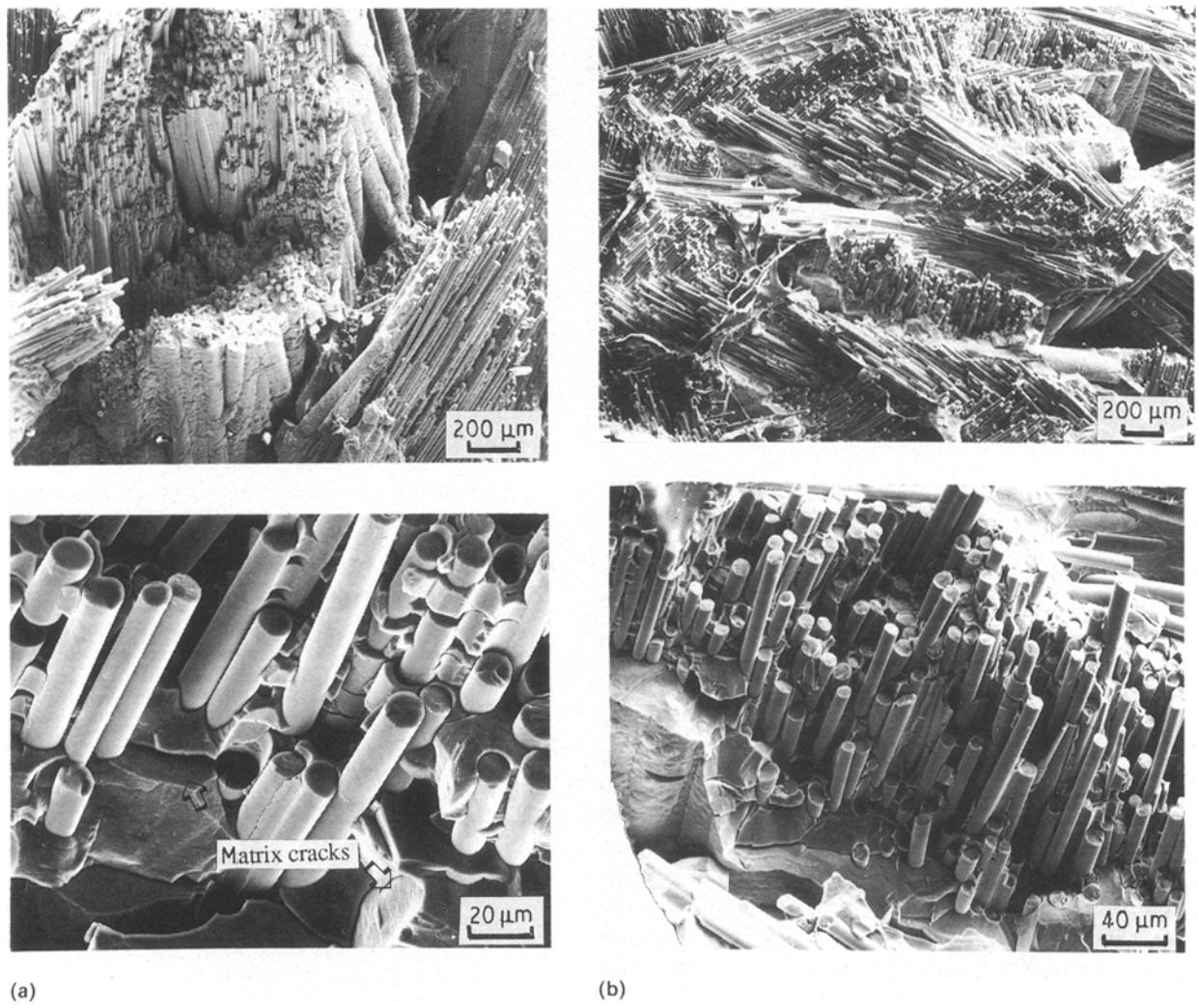

Figure 11 The fracture surface of (a) 3-D braided composite, (b) 2-D woven laminate subjected to impact loading.

side, and no delamination was found for either type of composite. For the 3-D braided composite, the crack propagates along the interface between fibre bundles which is a relatively weak region with no reinforcing fibres. The advancing crack was then deflected near the bundle cross-over due to the presence of matrix cracking and large voids. Serrated crack propagation patterns and extensive fibre bundle pull-out were observed for both four-point bending and single edge notched-beam specimens as shown in Fig. 8a. The toughening mechanism appears to be the crack deflection combined with fibre pull-out. For the 2-D woven laminate composite, slight crack serration due to the influence of the interlayer voids was observed. A minor amount of crack branching contributing further to the toughening was also observed. The advancing crack cut through the fill yarn bundles and split the warp yarn bundles as shown in Fig. 8b.

The extensive fibre pull-out indicates that a weak fibre/matrix bonding can be tailored through pyrolytic carbon coating. However, it has been found that the thickness of the carbon coating influenced the interfacial bonding and friction and, therefore, the matrix cracking stress and fracture behaviour of the composite [16]. In addition, the usefulness of the carbon coating is limited owing to its poor oxidation resistance at elevated temperatures. Further effort is needed to select a coating material which is inert to the fibres, and to understand the effects of the intermediate phase between fibres and matrix on the strength and toughness of the composite.

The results also indicate that the fibre placement will significantly affect the densification of the composites. Under the same processing conditions, the 3-D braided composite has fewer voids than the 2-D woven laminate composite. This is due to the nature of the braided structure which contains a more uniform pore network which would assist the diffusion of the gas reactants within the pore network. Microscopic examination reveals that most of the large pores were found either in between the fabric layers or in the bundle intertwined regions. More uniform preform structures with optimum bundle size and intratow spacing, as well as optimum weaving and braiding patterns should be developed in order to achieve a near full dense composite. Furthermore, the optimum CVI-processing conditions of temperature, pressure, gas flow rate, etc., need to be developed for each type of preform structure.

After thermal exposure at 1200 °C for 100 hours in an oxidizing environment, the strength and toughness of the 3-D braided and 2-D woven laminate composites dropped appreciably. However, as indicated in the stress–deflection curves, the composites still exhibited a non-catastrophic behaviour which is similar to that of the as-processed specimens. The property

degradation might be due to the changes in fibre/matrix bonding and fibre strength degradation. It has been found that, after exposure at high temperature in an oxidizing environment for a long period of time, the amorphous silica film on the Nicalon fibre will crystallize to α-crystabolite which undergoes a displacive transformation and volume decrease [17, 18]. Crack and debonding may then occur at the fibre/matrix interface. Fibre strength degradation is another factor which causes the reduction of properties after thermal exposure. It has been found that the Nicalon fibre is susceptible to decomposition, oxidation, accelerated grain growth and creep at high temperatures [19, 20]. A detailed analysis of the thermal degradation mechanisms is under investigation.

5. Summary

(1) The 3-D braided Nicalon/SiC composite, with its integrated fibre network, has a higher strength, better fracture resistance and damage tolerance than the 2-D woven laminate composite.

(2) The reduction in strength and toughness after thermal exposure at 1200 °C for 100 hours in an oxidizing environment might be due to the changes in fibre/matrix bonding conditions and fibre strength degradation.

(3) Further improvement in the performance of the composite can be achieved through designing the preform with optimum reinforcement geometry and pore structure, tailoring the interface chemistry, and optimizing the CVI parameters to further reduce the porosity.

Acknowledgements

This work was partially supported by the National Science Foundation (MSM-8809790)

References

1. D. P. STINTON, T. M. BESMANN and R. A. LOWDEN, *Ceram. Bull.* **67(2)** (1988) 130.
2. W. B. HILLIG, *Ann. Rev. Mater. Sci.* **17** (1987) 341.
3. R. COLMET, I. LHERMITTE-SEBIRE and R. NASLAIN, *Advanced Ceram. Mater.* **1** (1986) 185.
4. E. FITZER and R. GADOW, *Ceram. Bull.* **65(2)** (1986) 326.
5. R. NASLAIN and F. LANGLAIS, in "Tailoring multiphase and composite ceramics" (Plenum Press, New York, 1986) p. 145.
6. J. Y. ROSSIGNAL, J. M. QUENISSET and R. NASLAIN, *Composites* **18(2)** (1987) 135.
7. J. Y. ROSSIGNAL, J. M. QUENISSET, H. HANNACHE, C. MALLET, R. NASLAIN and F. CHRISTIN, *J. Mater. Sci.* **22** (1987) 3240.
8. J.-M. YANG, J. C. CHOU and C. V. BURKLAND, in "High temperature/high performance composites" (Materials Research Society, Pittsburgh, 1988) p. 163.
9. C. V. BURKLAND and J.-M. YANG, in Proceedings of NASA/DoD Conference on Metal, Ceramic and Carbon Matrix Composites, 1988.
10. C. V. BURKLAND, W. E. BUSTAMANTE, R. KLACKA and J.-M. YANG, in Whisker- and fiber-reinforced ceramics (ASM International, Metals Park, 1988), p. 225.
11. C. V. BURKLAND and J.-M. YANG, *SAMPE J.* **25(5)** (1989) 29.
12. J.-M. YANG, C. L. MA and T. W. CHOU, *J. Comp. Mat.* **20(5)** (1986) 472.
13. T. W. CHOU and J.-M. YANG, *Met. Trans.* **17A(9)** (1986) 1574.
14. F. K. KAO, *Ceram. Bull.* **68(2)** (1989) 401.
15. F. KO, M. KOZARK and G. LAYDEN, *Ceram. Eng. Sci. Proc.* **8(7–8)** (1987) 821.
16. R. A. LOWDEN, D. P. STINTON and T. M. BESMANN, in "Whisker- and fiber-reinforced ceramics" (ASM International, Metals Park, 1988) p. 187.
17. T. J. CLARK, M. JAFFE, J. RABE and N. R. LANGLEY, *Ceram. Eng. Sci. Proc.* **7(7–8)** (1986) 901.
18. L. C. SAWYER, R. T. CHEN, F. HAIMBACH, P. J. HARGET and J. JAFFE, *ibid.* **7(7–8)** (1986) 914.
19. T. J. CLARK, R. M. ARONS, J. B. STAMATOFF and R. RABE, *ibid.* **7(7–8)** (1985) 576.
20. T. I. MAH, M. G. MENDIRATTA, A. P. KATZ and K. S. MAZDIYASNI, Ceram. Bull. **66(2)** (1987) 304.

Received 13 March
and accepted 24 August 1989